Sliding Mode Control Optimized by Genetic Algorithm for Building Model

Hasan Omur Ozer*[,1], Alaattin Sayin[2], Nuray Korkmaz[3] and Nurkan Yagız[3]

[1]Programme of Air Conditioning and Refrigeration Technology, Vocational School of Technical Science, Istanbul University, 34320 Avcilar, Istanbul, Turkey
omurozer@yahoo.com
[2]Programme of Biomedical Equipment Tech., Vocational School of Technical Science, Istanbul University, 34320 Avcilar, Istanbul, Turkey
sayina@istanbul.edu.tr
[3]Department of Mechanical Engineering, Faculty of Engineering, Istanbul University, 34320 Avcilar, Istanbul, Turkey
nkorkmaz@istanbul.edu.tr

Abstract

Sliding Mode Control (SMC) has been used in many mechanical systems and structural system due to its robustness, simplicity and high control performance. However, choosing optimum parameters for systems is still an important research area. This study presents a numerical analysis to decrease the effect of earthquake vibrations on building model having Active Tuned Mass Damper (ATMD). The system is excited by an earthquake and a linear motor is used as the control device. ATMD is installed on top floor of building model. Tuning of Sliding Mode Controller (SMC) with Genetic Algorithm (GA) is designed for a three storey building model with ATMD. SMC parameters have been chosen by GA with a single objective function and a multiple objective function. Then, simulation results of uncontrolled and controlled model are compared. The results show that building model with SMC tuned by GA is effective to decrease the effects of earthquakes.

Keywords: Sliding mode controller, Genetic algorithm, Multi-objective genetic algorithm, Building model, Active tuned mass damper, Simulation of building vibration

https://krishtelemaging.in/Samples/jvet.pdf

1 Introduction

Many researches have been studied about controlling structural vibration due to potential failure risk or serious damage on buildings. Therefore, vibration control techniques have been improved recently.

The Tuned Mass Damper (TMD), invented in 1909, is a passive control system consisting of mass, springs and viscous dampers. Buildings are protected from hazardous effects of vibrations by using these systems. The optimum parameters of Tuned Mass Dampers (TMD) for different systems are proposed by several researchers; obtained optimum TMD parameters for complex Systems by Warburton and Ayorinde[1,2], gained optimum damper parameters with a frequency locus method by Thompson[3], suggested new approach for TMD by Villaverde[4–6], improved study of Vilaverde by Sadek[7]. Also, semi-active vibration methods are proposed in the literature. Yoshida and Fujio[8] applied a semi-active control method to a base in which the viscous damping coefficient is changed for vibration control. The numerical result indicates that efficiency of semi active TMD is better than conventional TMD, especially under the uncertainty of primary system[9].

Recent research and development activities in the field of vibration control are active vibration control systems emerged around 1970. These systems are active while resisting force exceeds the capacity of a passive-tuned-mass damper[10]. In order to control vibrations more effectively, numerous active control algorithms have been suggested. Guclu and Yazici[11] designed fuzzy logic and PD controllers for a multi-degree-of freedom structure with Active Tuned Mass Damper (ATMD) to suppress earthquake-induced vibrations. Yagiz[12] designed sliding mode control for controlling the vibration of multi-degree of freedom structures with an Active Tuned Mass Damper (ATMD) installed at the top floor to suppress earthquake or wind induced vibration. Essential requirements for sliding mode control are the hitting time reduction and chattering attenuation[13]. Bartolini[14], Bengiamin and Kauffmann[15] suggested inserting an integrator to the system to smooth the chattering but the system response was slow down. To manage the chattering problem, Hwang and Lin[16], Lin and Chen[17] applied the fuzzy set theory. Pourzeynali *et al.*[18] was suggested that integration of the GAs and fuzzy logic controller to obtain optimum values of ATMD is highly effective in reduction of seismically excited building.

This study presents a numerical analysis to decrease the effect of earthquake vibrations on building model having Active Tuned Mass Damper (ATMD). To select suitable gain switching and sliding surface parameter is significant for system performance. The searching of these parameters has been done by two different fitness functions with Genetic Algorithm. Sliding Mode Controller (SMC) tuning with Genetic Algorithm (GA) are designed for a three storey building model with ATMD. The simulation results of uncontrolled and controlled model are compared.

*Corresponding author.

2 Building Model with ATMD

The building model has three degree of freedom (Fig. 1). ATMD has been placed on top floor of the building model. m_i, k_i and $b_i (i = 1, 2, 3)$ denotes the mass, stiffness and damping values related to each storey of the building model and m_4, k_4 and b_4 stand for the mass, stiffness and damping values of the ATMD respectively.

The mathematical model of the three-storey building model with ATMD has obtained using Lagrange's equations and presented (1). The system has been excited by El-Centro earthquake

$$[M]\ddot{x}_i(t) + [B]\dot{x}_i(t) + [K]x_i(t) = P_i(t) \tag{1}$$

$$x(t) = \begin{bmatrix} x_1 & x_2 & x_3 & x_4 \end{bmatrix}^T \tag{2}$$

Mass, stiffness and damping matrix is shown in (3–5).

$$[M] = \text{diag}\begin{bmatrix} m_1 & m_2 & m_3 & m_4 \end{bmatrix} \tag{3}$$

$$[B] = \begin{bmatrix} b_1 + b_2 & -b_2 & 0 & 0 \\ -b_2 & b_2 + b_3 & -b_3 & 0 \\ 0 & -b_3 & b_3 + b_4 & -b_4 \\ 0 & 0 & -b_4 & b_4 \end{bmatrix} \tag{4}$$

$$[K] = \begin{bmatrix} k_1 + k_2 & -k_2 & 0 & 0 \\ -k_2 & k_2 + k_3 & -k_3 & 0 \\ 0 & -k_3 & k_3 + k_4 & -k_4 \\ 0 & 0 & -k_4 & k_4 \end{bmatrix} \tag{5}$$

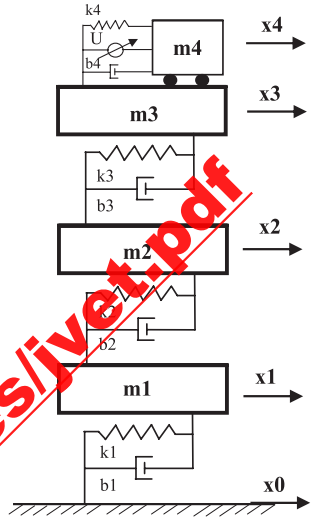

Fig. 1 The psychical model of building model

A linear motor is used as the control device. Linear motor force F_u has been calculated using (6) and (7) as shown in (8)

$$Ri + K_e(\dot{x}_4 - \dot{x}_3) = u \tag{6}$$

$$F_u = K_f i \tag{7}$$

$$F_u = (K_f/R)u - (K_e K_f/R)(\dot{x}_4 - \dot{x}_3) \tag{8}$$

$$E_{\text{ATMD}} = F_u(t)\Delta x_4 \tag{9}$$

External loads have consisted of earthquake force and control force shown in (10)

$$[P] = \begin{bmatrix} -m_1\ddot{x}_0 & -m_2\ddot{x}_0 & -m_3\ddot{x}_0 - F_u & -m_4\ddot{x}_0 + F_u \end{bmatrix}^T \tag{10}$$

3 Parameter Selection for Building Model

The mass and stiffness parameters of the building model have been taken from study of Sadek[7]. The damping parameters have been derived from $C = (0.0129)K$[19] and the parameter of the ATMD has been shown Tables 1–2.

Table 1 Ratios for building model (adapted from Sadek[7])

Number of Floors	Mass Ratio	Tuning Ratio (f)	TMD Damping Ratio (ξ)	$M_1 = \Phi_1^T[M]\Phi_1$ (10^3 kg)	ω_{01} (Hz)
3	0.100	0.8701	0.3694	271	1.41

Table 2 Parameters of building model with ATMD (adapted from Sadek[7])

Floor	Mass (10^3 kg)	Stiffness (kN/m)	Damping Coefficient (kNs/m)
1	100	41000	528.9
2	100	38000	490.2
3	100	36000	464.4
ATMD	27.1	1610.73	154.35

https://krishtelemaging.in/Samples/jvet.pdf

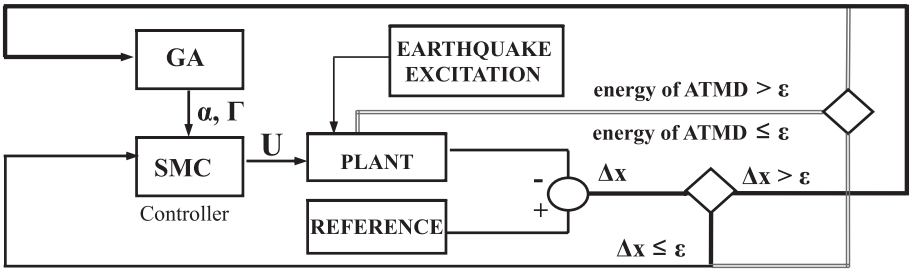

Fig. 2 The flowchart of control algorithm

4 Control Strategy

4.1 Sliding mode control

Sliding Mode Control is a variable structure control method. Sliding controller design provides a systematic approach to the problem of maintaining stability and consistent performance in the face of modeling imprecision[20]. Sliding mode control theory has been applied to many nonlinear systems. The main idea is to bring and keep the error on a sliding surface such that the system is insensitive to the disturbances and parameter changes[21,22]. Sliding surface can be chosen as (11). Δx is error matrix. $[G]$ contains gradient of sliding surface

$$\sigma = [G][\Delta X] = \underbrace{[G][X_r]}_{A} - [G][X] \tag{11}$$

A Lyapunov function is chosen and must have a value greater than zero, whereas its derivative should be smaller than zero

$$V(\sigma) = (\sigma^T \sigma)/2 > 0 \quad \dot{V}(\sigma) = \sigma^T \dot{\sigma} \leq 0 \tag{12}$$

According to limit situation can be calculate control input in sliding surface

$$\dot{\sigma} = \frac{d[A]}{dt} - [G]\{f(x) + [B]u\} = 0 \Rightarrow u_{eq} \tag{13}$$

$$\dot{\sigma} = -[\Gamma](\sigma) \Rightarrow u \tag{14}$$

$$\underbrace{[GB]^{-1}\left\{\frac{d[A]}{dt} - [G][f(x)]\right\}}_{u_{eq}} + [GB]^{-1}[\Gamma](\sigma) = u \tag{15}$$

Suggested that the equivalent control is the average of the total control[23] an averaging filter is used for calculation. The equivalent control is shown in (16)

$$\hat{u}_{eq} = \frac{1}{\tau s + 1} u \tag{16}$$

$$u = \hat{u}_{eq} + [GB]^{-1}[\Gamma](\sigma) \tag{17}$$

The system must be defined in state space form as $\dot{x} = f(x) + [B]\underline{u} + [C]\underline{w}$

$$\begin{bmatrix} X_1 & X_2 & X_3 & X_4 & X_5 & X_6 & X_7 & X_8 & X_9 & X_{10} & X_{11} & X_{12} \end{bmatrix}^T$$
$$= \begin{bmatrix} x_1 & x_2 & x_3 & x_4 & \dot{x}_1 & \dot{x}_2 & \dot{x}_3 & \dot{x}_4 & x_0 & \dot{x}_0 & U & \ddot{x}_0 \end{bmatrix}^T \tag{18}$$

https://krishtelemaging.in/Samples/jvet.pdf

$$\begin{bmatrix}\dot{X}_1\\ \dot{X}_2\\ \dot{X}_3\\ \dot{X}_4\\ \dot{X}_5\\ \dot{X}_6\\ \dot{X}_7\\ \dot{X}_8\end{bmatrix} = \begin{bmatrix} X_5 \\ X_6 \\ X_7 \\ X_8 \\ ((-k_1-k_2)/m_1)X_1 + (k_2/m_1)X_2 + ((-b_1-b_2)/m_1)X_5 + (b_2/m_1)X_6 \\ (k_2/m_2)X_1 + ((-k_2-k_3)/m_2)X_2 + (k_3/m_2)X_3 \\ +(b_2/m_2)X_5 + ((-b_2-b_3)/m_2)X_6 + (b_3/m_2)X_7 \\ (k_3/m_3)X_2 + ((-k_3-k_4)/m_3)X_3 + (k_4/m_3)X_4 + (b_3/m_3)X_6 \\ + \left(\left(-b_3-b_4-\frac{K_eK_f}{R}\right)\Big/ m_3\right)X_7 + \left(\left(b_4+\frac{K_eK_f}{R}\right)\Big/ m_3\right)X_8 \\ (k_4/m_4)X_3 + (-k_4/m_4)X_4 + \left(\left(b_4+\frac{K_eK_f}{R}\right)\Big/ m_4\right)X_7 + \left(\left(-b_4-\frac{K_eK_f}{R}\right)\Big/ m_4\right)X_8 \end{bmatrix}$$

$$+ \begin{bmatrix}0\\0\\0\\0\\0\\0\\-K_f/Rm_3\\K_f/Rm_4\end{bmatrix}[u] + \begin{bmatrix}0\\0\\0\\0\\(b_1/m_1)X_{10} + (k_1/m_1)X_9 - X_{12}\\-X_{12}\\-X_{12}\\-X_{12}\end{bmatrix}[w] \tag{19}$$

$$[G] = \begin{bmatrix}0 & 0 & \alpha & 0 & 0 & 0 & 1 & 0\end{bmatrix} \tag{20}$$

The control law can be shown in (21)

$$[u] = \hat{u}_{eq} - \frac{Rm_3}{K_f}[\Gamma]\left\{\alpha \underbrace{(X_{3r} - X_3)}_{e} + \underbrace{(X_{7r} - X_7)}_{\dot{e}}\right\} \tag{21}$$

4.2 Sliding mode control parameters tuned by genetic algorithm

Genetic Algorithms (GAs) used principles inspired by genetic processes occurring in nature to evolve solutions to problems. GAs usually consist of reproduction, crossover and mutation operators. A fitness function must be devised for each problem to be solved[18]. While the fitness function is minimum, the optimum SMC parameters will be obtained.

The aim of Multi-Objective Optimization with Genetic Algorithm is minimization of multiple fitness function simultaneously. The multi objective genetic algorithm is used to solve multi objective optimization problems by identifying the Pareto front - the set of evenly distributed non dominated optimal solutions[24, 25].

The proposed method can efficiently choose the appropriate gain parameters α, Γ for sliding mode controller based on two proposed fitness functions. First fitness function is devised to obtain maximum reduction in the third floor response. The aim of the second fitness function is minimizing the control energy and also minimizing third floor's response quantity. GA is implemented for tuning of the parameters of sliding mode controller. The optimum value of gain parameters α, Γ obtained by GA is used to simulated structural system. The flowchart of the control algorithm is shown as Fig. 2.

5 Simulation Results

5.1 GA's fitness function

The value of minimized third floor's response is scanned by Genetic Algorithm. The fitness function is as below

$$\phi_1(\alpha, \Gamma) = \sum_{ti}^{tf} e(t) = \sum_{ti}^{tf}[x_{3r}(t) - x_3(t)] \tag{22}$$

The optimum value of α, Γ is [125 127]. Maximum reduction in the building response has been obtained but the value of the control force may have been considerably high. The results are shown in Table 3 and Table 4. Total energy consumed by ATMD is 3586.75 kJ with the parameters.

https://krishtelemaging.in/Samples/jvet.pdf

In-Situ Measured Vibration behavior of a Steam Turbine

Wolfgang Hahn[1] **and Jyoti K. Sinha**[2,*]

[1]EDF Energy, West Burton Power Station, Nottinghamshire DN22 9BL UK
Wolfgang.hahn@edfenergy.com
[2]School of MACE, The University of Manchester, Manchester M13 9PL, UK
Jyoti.Sinha@manchester.ac.uk

Abstract

Cracking of a few last stage blades of the Low Pressure (LP) turbines is observed in a typical steam Turbo-Generator (TG) unit at the West Burton Power Plant UK. In-situ vibration measurements are carried out during the steady state operation at different power generation outputs. A typical phenomenon of appearance of low frequencies in band of 7–12 Hz is observed mainly related to the vibration measurements on LP turbines. This band of frequency observed to be modulating with vibration at the machine RPM (50 Hz) and its higher harmonics. The appearance of such behavior often related to the stall phenomena which generally has high potential of damage. The paper presents the observations, results and the possibility of stall in the LP turbines.

Keywords: Steam turbine, LP blade cracking, Vibration measurement, Vibration spectrum, Rotor stall

https://krishtelemaging.in/Samples/jvet.pdf

1 Introduction

West Burton Power Plant, UK owned by EDF Energy has 4 steam Turbo-Generator (TG) units for the power generation. Each TG unit consists of a High Pressure (HP) turbine, an Intermediate Pressure (IP) turbine and three Low Pressure (LP) turbines together with a generator and an exciter. The photograph of the TG unit is shown in Fig. 1. These units were installed and commissioned between 1967 and 1969 and since then operated smoothly without any major problems up to 2007. In 1994 and 1995, the two TG sets, namely Unit 2 and 3, were retrofitted with the new design LP rotor including blades and in 2007 and 2008, retrofitting of HP turbines in all 4 units was commenced. The retrofitting was done without changing the foundation, but only with the aim to enhance the power output by 20 MW and increased efficiency.

The upgraded and retrofitted 2 TG units have been suffering from blade vibration problems in stages 3, 4 and 5 on the LP turbines and blade cracking in the last stage blades. These turbines have been suffering with erosion and last stage blade cracking which became more prominent after 2007, since the HP turbines were retrofitted. The cracking in the turbine blades have been found just above the blade root which is expected to be high stress location for the first bending mode for the blade. The last stage bladed disc is shown in Fig. 2. Typical blades with erosion and with crack are shown in Fig. 3. The blade erosion and then crack propagation is suspected as a result of blade excitation during the normal and transient (run-up

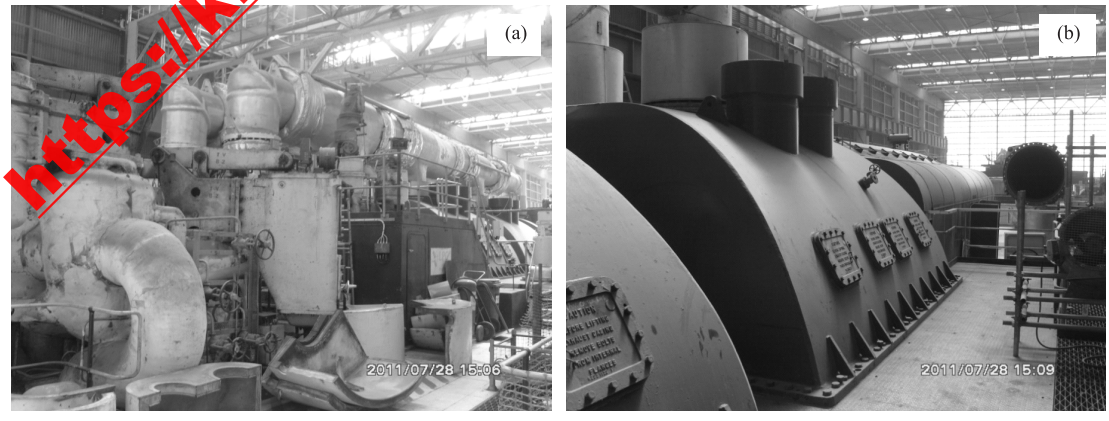

Fig. 1 Typical photograph of TG set, (a) HP-IP turbines, (b) LP turbines and generator

*Corresponding author.

or run-down) operations[1]. The in-situ Blade Tip Timing (BTT) measured data on the last stage blades (steam side) of the Unit 3 LP1 turbine also confirm the high vibration amplitude of a few blades which could cause the blade cracking[2].

In-situ vibration measurements are carried out on the Unit 3 during the steady state operation at different power generation outputs to understand the machine vibration behavior. A typical phenomenon of appearance of low frequencies in band of 8–12 Hz is observed mainly related to the vibration measurements on LP turbines. This band of frequency observed to be modulating with vibration at the machine RPM (50 Hz) and its higher harmonics. The appearance of such behavior often related to the stall phenomena[3–9] which generally has high potential of damage. The paper presents the typical observations, results and the possibility of stall in the LP turbines.

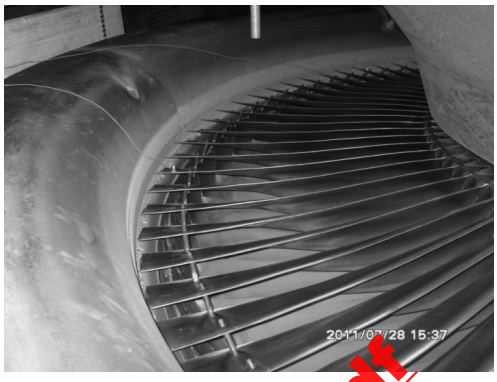

Fig. 2 Typical LP1 last stage from bladed disc (new design blades) near IP turbine (steam end)

2 Machine Critical Speeds and LP Turbine Blades Natural Frequencies[1]

Earlier study[1] and vibration measurements during machine transient operations (rundown and runup) suggests that the machine critical speeds are 27.34 Hz, 33 Hz, 40.50 Hz and 46.88 Hz upto machine 3000 rpm. Similarly the experimentally identified first 3 natural frequencies are in the frequency range of 62.87–64.70 Hz, 116.6–119.0 Hz and 247.8–250.9 Hz respectively. Modal tests are conducted when machine was completely at stand still condition (zero machine RPM). The frequency range at each natural frequency of the blades indicates the small scatter in natural frequencies from blade-to-blade. It is likely that the first natural frequency of the LP last stage blades may be around 80–90 Hz at machine 3000 rpm due to the stiffening effect by the centrifugal force. These data are important for the present study.

3 Vibration Measurements

A simple schematic of the TG set is shown in Fig. 4. A total of 14 numbers of fluid bearings in each TG unit are used in a TG unit to support the rotors of the steam turbines, generator and exciter. The measurements are done at the bearing housings for bearings mainly in the vertical direction and also in the horizontal direction at the bearing B5 and B6. Accelerometers of sensitivity 100 mV/g with linear frequency measurement range up to 10 kHz are used. The vibration data are then collected and stored in the PC through 16 channels 16-bit data acquisition analogue to digital device for further signals processing. Table 1 gives the summary of measurements dates and times including power generation, LP turbine exhaust steam temperatures, condenser vacuum pressure and observations during the vibration measurements.

https://krishtelemaging.in/Samples/jvet.pdf

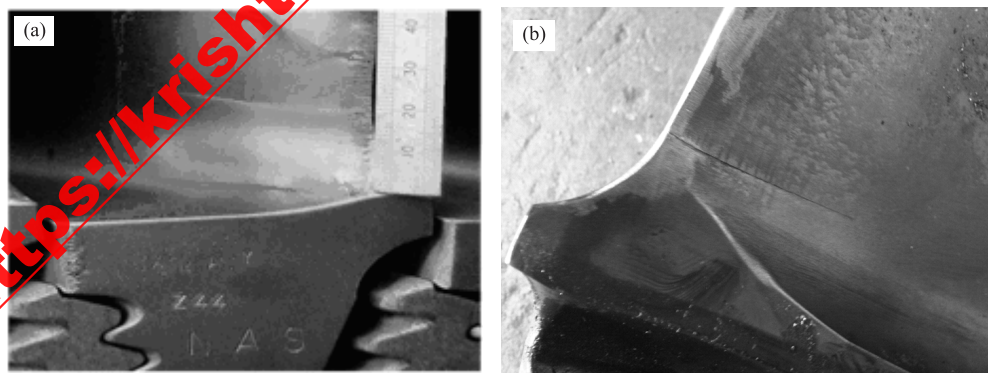

Fig. 3 Typical LP last stage blades, (a) showing erosion marks, (b) crack in a blade

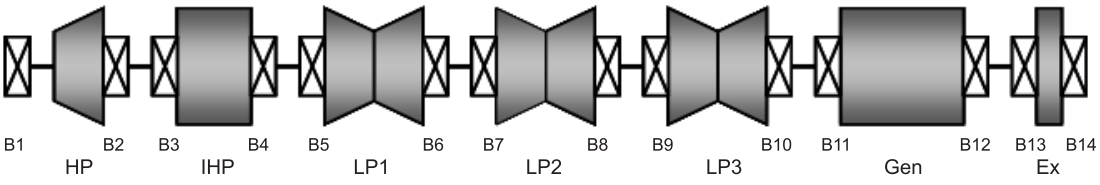

Fig. 4 A simple schematic of TG unit

Table 1 Summary of measurements with observations

No	Date	Time H:M	Power MW	TURBINE LP EXHAUST TEMPERATURES						CONDENSER VACUUM mbar	OBERVATIONS
				LP1 STEAM END	LP1 GEN END	LP2 STEAM END	LP2 GEN END	LP3 STEAM END	LP3 GEN END		
1	16 FEB. 2011	16:23	516.22	31.01	33.69	29.161	30.72	29.80	31.40	47.7	7-12Hz and its modulation at 50Hz, 100Hz, etc.
2	16 FEB. 2011	21:33	515.72	28.84	30.92	27.14	28.35	28.30	29.43	45.1	7-12Hz and its modulation at 50Hz, 100Hz, etc.
3	17 FEB. 2011	05:49	187.47	21.80	22.80	23.00	22.50	23.10	23.90	26.9	No appearance of 7-12Hz
4	17 FEB. 2011	07:07	426.52	24.97	25.78	24.39	23.90	25.15	26.35	34.3	No prominent 7-12Hz and its modulation
5	17 FEB. 2011	20:35	516.54	29.66	30.56	27.08	28.09	27.96	29.32	44.1	7-12Hz and its modulation at 50Hz, 100Hz, etc.
6	18 FEB. 2011	06:42	120	21.10	22.80	21.20	22.20	21.70	24.10	28.90	Negligible 7-12Hz and its modulation at 50Hz, 100Hz, etc.

4 Spectrum Analysis

The spectrum analysis of all the measured vibration data in Table 1 are compared initially to understand the vibration behavior of the TG set (Unit 3). It is observed that TG unit has in general strong peaks at 1x (1 times RPM) and 2x (2 times RPM) at all the bearings. This indicates there could be some misalignment in the shafts of HP, IP, LP turbines and the generator rotors. Typical vibration spectra in contour form at bearing B5 in the vertical direction are shown in Fig. 5. Further inspection of spectra also indicates a presence of frequency peaks of 7–12 Hz and this frequency band gets modulated with 50 Hz (1x) and higher harmonics. The averaged spectrum is also computed for all data with the frequency resolution of 0.24 Hz with 90% overlap from the measured vibration data of 20 s data length. A few typical averaged spectra for the different measurement dates-times and power generation as per Table 1 are also shown in Figs. 6–11. It is clear from the spectra that the existence and the modulation of 7–12 Hz in several occasions during machine operation. These observations are also summarized in Table 1. This effect is generally prominent in the LP turbines and often not in the HP-IP turbines (see Fig. 12) and the generator.

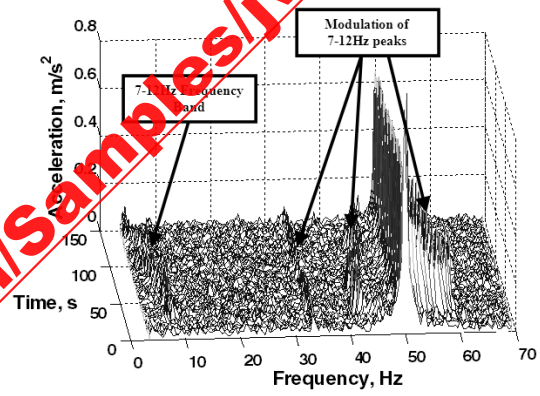

Fig. 5 Typical waterfall diagram of the measured acceleration vibration spectra at the bearing B5 in vertical direction

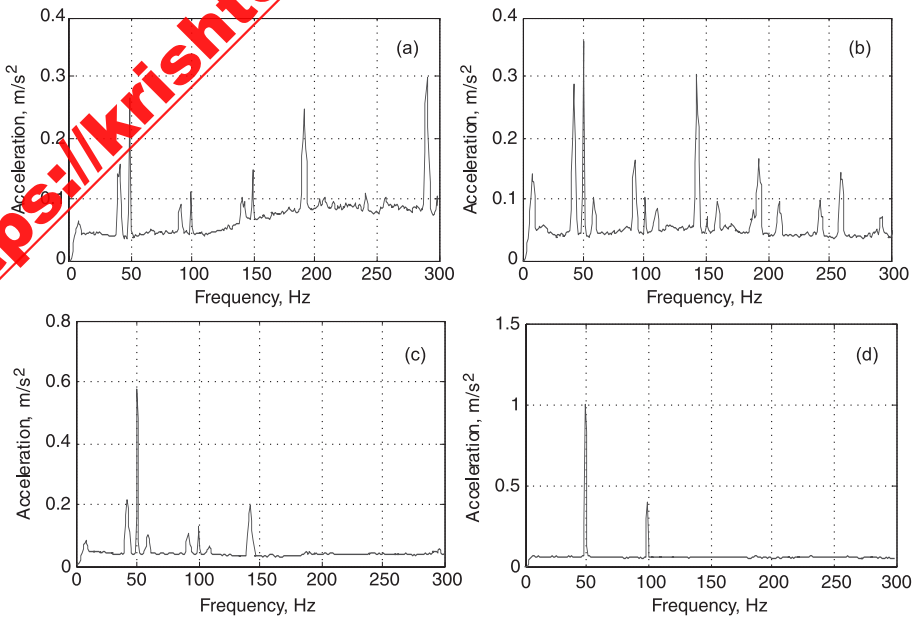

Fig. 6 Measured vibration spectra at the bearing pedestals in the vertical direction on 16th February 2011 at time 16:23, (a) B5, (b) B7, (c) B9, (d) B11

https://krishtelemaging.in/Samples/jvet.pdf

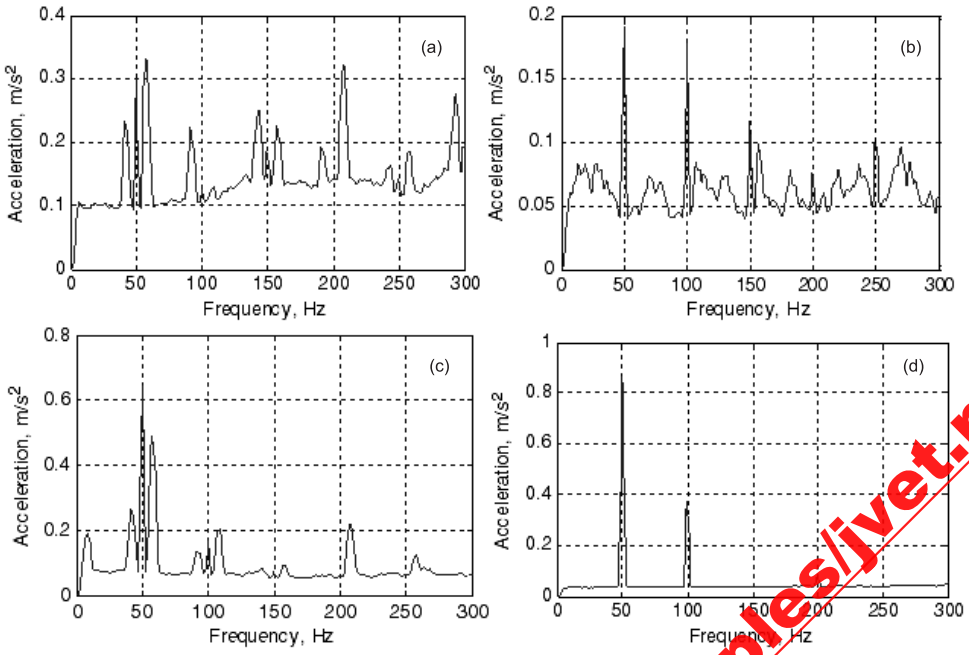

Fig. 7 Measured vibration spectra at the bearing pedestals in the vertical direction on 16th February 2011 at time 21:33, (a) B5, (b) B7, (c) B9, (d) B11

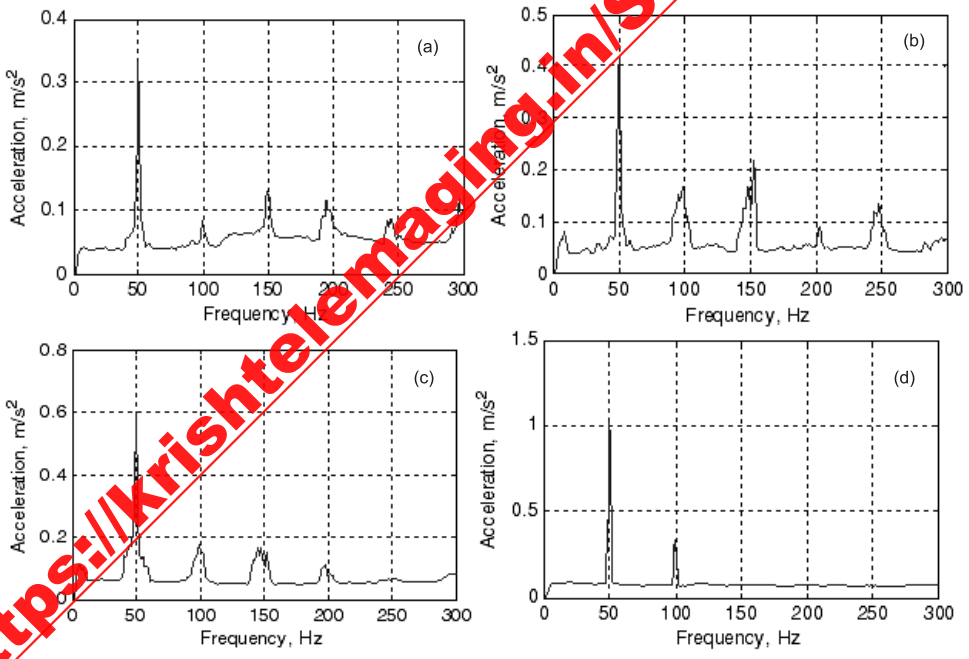

Fig. 8 Measured vibration spectra at the bearing pedestals in the vertical direction on 17th February 2011 at time 5:49, (a) B5, (b) B7, (c) B9, (d) B11

https://krishtelemaging.in/Samples/jvet.pdf

5 Possible Stall Phenomenon

The phenomenon of low frequency 7–12 Hz peak and its modulation with the 1× and higher harmonic components is not a usual feature for the steam turbine. It is also important to note that it is not exiting continuously and not clearly observed in the HP-IP turbines and the generator. The phenomenon is often intermittent and may be depending upon several operating parameters and possibly related with the LP turbines.

Often the fluid induced instability in the fluid bearing generates a frequency peak below sub-harmonic frequency $(0.5x)$[3], however the present observations are much different. The experimental study on a compressor by Bently *et al.*[4] suggests that this phenomenon could be related to the rotating stall which may often have potential for any damage. The features in the spectrum by Bently *et al.*[4] in Fig. 13 are nearly same as the present observations shown in Fig. 6. This comparison